Electrocatalysis

DOI: 10.1002/ange.201205314

Design of an Active Site towards Optimal Electrocatalysis: Overlayers, Surface Alloys and Near-Surface Alloys of Cu/Pt(111)**

*Aliaksandr S. Bandarenka, Ana Sofia Varela, Mohammedreza Karamad, Federico Calle-Vallejo, Lone Bech, Francisco J. Perez-Alonso, Jan Rossmeisl, Ifan E. L. Stephens, and Ib Chorkendorff**

Electrochemical devices hold promise as a sustainable route for energy conversion to meet the requirements of future generations. Their development is contingent upon improvements to the functionality of their electrodes.[1] The catalytic performance of these materials is controlled by the atomic and electronic structure of their active sites.[1b,2] Therefore, the design of the appropriate active site is crucial to obtain high catalytic activity, especially where multi-functionality is needed. However, the control of a given surface on an atom-by-atom basis is particularly challenging.

The electrochemical oxidation of CO is the prototypical bifunctional reaction.[3] The active site needs to be reactive towards both oxygen and carbon atoms. Because Pt is reactive towards carbon atoms and Cu is reactive towards oxygen atoms,[4] these are two obvious candidates for the construction of a bifunctional catalyst for electrochemical CO oxidation.

Fundamental studies have shown that overlayers (OLs), near-surface alloys (NSAs), and surface alloys (SAs) of Cu/Pt show markedly different characteristics from pure Cu or Pt surfaces.[5] Herein, we present a study of how to control the reactivity of the Cu/Pt(111) system by modifying the atomic structure in an electrochemical environment. We employ electrochemical measurements, angle-resolved X-ray photoelectron spectroscopy (AR-XPS), and density functional theory (DFT) calculations. This has allowed us to make a detailed comparison between experimental results and theoretical simulations on identical systems.

The Cu/Pt(111) OL, SA, and NSA were prepared according to the general method shown in Figure 1. The resulting AR-XPS depth profiles in Figure 1 confirm that the desired structures were formed.[5c]

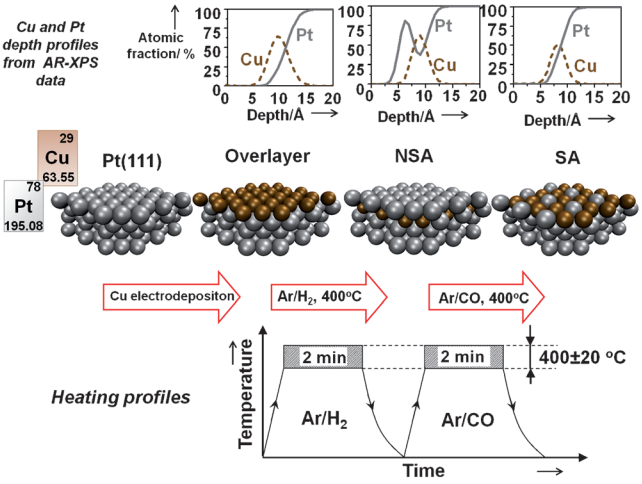

Figure 1. General scheme used to prepare Cu/Pt(111) OL, NSA, and SA. The corresponding depth profiles, obtained using AR-XPS, are shown at the top.

There are considerable differences between the voltammograms of the surfaces in 0.1 M $HClO_4$, as shown in Figure 2. On Pt(111), from 0.05 V to 0.4 V there is a reversible peak arising from the adsorption/desorption of *H (herein * denotes a free site and *X an adsorbed species, X); from 0.6 V to 0.9 V there is a reversible peak arising from the adsorption of *OH.[6] On the NSA, the *H peak is shifted negatively and the *OH peak is shifted positively, suggesting that both *H and *OH are destabilized,[5c] consistent with our DFT calculations, described in the Supporting Information. On the other hand, the Cu/Pt(111) overlayer exhibits a featureless voltammogram between 0.05 V and 0.38 V (the potential was limited to this range because above 0.38 V there was a small oxidation current, prior to the main peak at 0.7 V, as shown in the inset in Figure S5a of the Supporting Information; this could be attributed to Cu dissolution). According to our *CO-displacement measurements (see

[*] Dr. A. S. Bandarenka, A. S. Varela, Dr. L. Bech, Dr. F. J. Perez-Alonso, Dr. I. E. L. Stephens, Prof. I. Chorkendorff
Center for Individual Nanoparticle Functionality
Technical University of Denmark, Building 312
DK-2800 Lyngby (Denmark)
E-mail: ibchork@fysik.dtu.dk
Homepage: http://www.cinf.dtu.dk
M. Karamad, Dr. F. Calle-Vallejo, Dr. J. Rossmeisl
Center for Atomic-Scale Material Design
Technical University of Denmark, Building 307
DK-2800 Lyngby (Denmark)
Dr. A. S. Bandarenka
Center for Electrochemical Sciences, Ruhr Universität Bochum
Universitätsstrasse 150 NC 4/73, 44801 Bochum (Germany)

[**] Funding by the Danish Strategic Research Council's (DSRC) HyCycle program and SERC project (grant no. 2104-06-0011), the Spanish Government's, "Programa Nacional de Movilidad de Recursos Humanos del PN de I-D + I 2008-2011", the PSO-financed ForskEL/ELgrant (HighPerformanceMEA's, project 010076) from energinet.dk and Catalysis for Sustainable Energy research initiative, funded by the Danish Ministry of Science Technology and Innovation is acknowledged. A.S.B. acknowledges additional financial support from the European Union and the MWIFT-NRW (Hightech.NRW competition). The Center for Atomic-scale Materials Design is supported by the Lundbeck Foundation. The Center for Individual Nanoparticle Functionality is supported by the Danish National Research Foundation.

Supporting information (experimental details) for this article is available on the WWW under http://dx.doi.org/10.1002/anie.201205314.

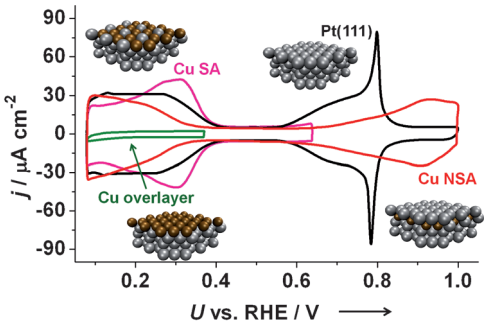

Figure 2. Cyclic voltammograms in 0.1 M $HClO_4$ of: Pt(111), Cu OL on Pt(111), Cu/Pt(111) NSA, and Cu/Pt(111) SA. $dU/dt = 50\ mV s^{-1}$.

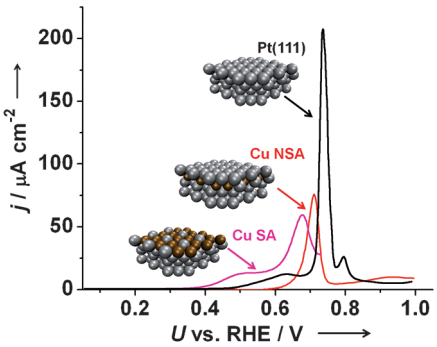

Figure 3. *CO stripping voltammograms for Pt(111), Cu/Pt(111) SA, and Cu/Pt(111) NSA, in $HClO_4$, $dU/dt = 20\ mV s^{-1}$. The CO was adsorbed at 0.05 V, whereas the voltammogram was carried out in a CO-free solution.

Supporting Information), the surface is covered with anionic species in this potential range, which our DFT calculations suggest should be *OH. Within the short time required for a voltammogram, no further anion adsorption takes place, explaining the absence of any peaks. On the other hand, the Cu/Pt(111) SA voltammogram has a reversible peak centered at 0.3 V. The DFT calculations would suggest that this is due to the adsorption of *OH on the Cu sites: *OH binds the SA 0.6 eV stronger than Pt(111), in good agreement with the approximate shift of 0.5 V between the peak on the SA and that of *OH adsorption on Pt(111).

Our results confirm that the trends observed previously for the gas-phase adsorption of *CO[5a,b] also persist for the electrochemical adsorption of *H and *OH (consistent with similar investigations by others,[7] there is a linear correlation between the binding energies of *CO and *H, as shown in Figure S4). Placing Cu in the first atomic layer, as in the SA, results in stronger interactions with *H and *OH, whereas placing Cu in the second layer, as in the NSA, weakens the interaction with the same adsorbates. Having established the relationship between the position of Cu and the reactivity of the surface, we will now use this relationship to control the activity for an electrocatalytic reaction: CO adlayer oxidation.

The *CO electro-oxidation voltammogram for Pt(111), Cu/Pt(111) SA, and NSA is shown in Figure 3. The observed area of the CO electro-oxidation peaks can be used to estimate the CO coverage of each surface. For Pt(111), the charge of $328\ \mu C cm^{-2}$ corresponds to a coverage of 0.68 monolayers (ML), consistent with 0.7 ML obtained by DFT calculations (Supporting Information) and with previous results.[8] In contrast, the charge of $164\ \mu C cm^{-2}$ on the NSA corresponds to a coverage of 0.34 ML, which is in good agreement with the sharp change in CO differential free energy of adsorption at a coverage of 0.33 ML predicted by DFT (Figure S1 b). Because both consist of pure Pt atoms in the outer layer, the difference in *CO coverage can only be attributed to the modified electronic properties of the Pt surface atoms. It is interesting to compare the Cu/Pt(111) NSA with $Pt_3Ni(111)$ and $Pt_3Co(111)$, both of which also have first layers of pure Pt atoms.[9] On these bulk alloys, the coverage of *CO approximates that of Pt(111). This is clearly not the case for the NSA, suggesting that the CO electro-oxidation charge may not always provide a one-to-one correlation with the surface area of nanocatalysts with a Pt overlayer.

For the SA, there is also an abrupt change in the calculated CO differential free energy of adsorption when the coverage reaches 1/3 ML, suggesting that this is the equilibrium coverage (Figure S1 a). This is consistent with a CO molecule covering each platinum surface atom. However, the rigorous experimental determination of the *CO coverage is challenging; the charge owing to CO electro-oxidation is convoluted with the charge arising from *OH adsorption and Cu dissolution (which starts above 0.7 V).

We compare the catalytic activity of the different surfaces towards CO electro-oxidation by taking into account the position of the main peak, corresponding to terrace-bound *CO.[8] The potential required to oxidize CO increases in the following order: SA < NSA < Pt(111).

To understand this reaction, we consider the following mechanism [Eq. (1)–(3)]:

$$CO(g) + * \rightarrow *CO \quad (1)$$

$$H_2O(l) + * \rightarrow *OH + H^+(aq) + e \quad (2)$$

$$*OH + *CO \rightarrow CO_2 + H^+(aq) + e^- + 2* \quad (3)$$

Applying a Sabatier analysis,[10] the optimal catalyst for the electrochemcial oxidation of CO must have an intermediate binding energy towards both *CO and *OH.[9]

Figure 4 shows the 3D volcano plot for CO electro-oxidation as a function of the free energies of adsorption of *CO and *OH. In agreement with our experiments, the overpotential required to oxidize CO increases in the following order: SA < NSA < Pt(111). The SA exhibits a lower overpotential for CO oxidation by virtue of its bifunctional nature: *OH binds to Cu sites and *CO binds to Pt.

Strikingly, the volcano plot suggests that the Cu/Pt(111) OL should exhibit optimal activity for *CO electro-oxidation. However, this theoretical prediction could not be realized, since the Cu overlayer is destabilized by the presence of CO.[11] This caused the oxidation of *CO to be accompanied by the dissolution of the Cu (see Supporting Information).

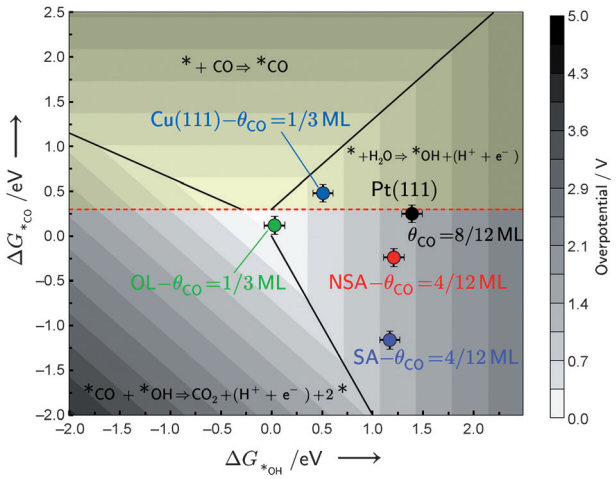

Figure 4. Volcano plot for CO electro-oxidation as a function of the differential free energies of adsorption of CO and OH on different surfaces: Pt(111), Cu(111), Cu/Pt(111) NSA, Cu/Pt(111) SA, and Cu/Pt(111) OL. ΔG_{*CO} is the differential free energy of adsorption of CO when the surfaces are pre-adsorbed with CO, near the corresponding saturation coverage. ΔG_{*OH} is the differential free energy of adsorption of OH co-adsorbed with *CO. The coverage of CO is depicted for each surface. The potential determining step for each region is also defined. The dashed horizontal line denotes the chemical potential of CO in the gas phase, above which CO does not bind to the surface (yellow region).

This illustrates that optimal binding to the intermediates is a necessary but insufficient criterion for an effective catalyst: it must also be stable.[12]

In the NSA, subsurface Cu is kinetically stable below 1.15 V. However, both the SA and the OL are unstable at potentials more positive than 0.7 V, as shown in Figure S5; this observation is consistent with the DFT-calculated dissolution potentials, which are roughly equal for the SA and the OL, as documented in Table S1. Thus the position of the solute metal determines its stability. Less noble metals, which are often alloyed with Pt, such as Ni, Co, Fe, La, or Y, have much lower dissolution potentials than Cu.[13] On the basis of our results, we would not expect these reactive metals to be stable at high potentials in the first surface layer, in contrast to some reports in the literature.[14] The kinetic stability of the solute metal is contingent upon a protective Pt overlayer.

In conclusion, our results demonstrate an unprecedented degree of agreement between electrochemical experiments and first-principle calculations. The location of Cu atoms in Pt(111) controls its interaction with *H, *OH, and *CO. Weakening the binding of CO, by forming a subsurface alloy, can decrease the saturation coverage of CO; thus the CO oxidation charge may not always be a reliable method for the determination of the surface area of nanocatalysts with Pt overlayers. In contrast, Cu atoms in the first layer strengthen the Pt binding energy towards *H, *OH, and *CO. Using this knowledge, we tailored the configuration of Cu atoms in Pt(111) for the electro-oxidation of CO. A large number of electrochemical processes for sustainable fuel production and utilization are controlled by the binding to these adsorbates.[5c,10b,15] Our general approach, outlined here, could enable further progress to be made to the catalysis of these all-important reactions.

Received: July 5, 2012
Published online: October 22, 2012

Keywords: Cu/Pt alloy · cyclic voltammetry · density functional calculations · electrocatalysis · electrochemistry

[1] a) H. A. Gasteiger, J. Garche in *Handbook of Heterogeneous Catalysis*, 2nd ed. (Eds.: G. Ertl, H. Knoezinger, F. Schueth, J. Weitkamp), Wiley-VCH, Chichester, **2008**, pp. 3081–3120; b) D. V. Esposito, S. T. Hunt, A. L. Stottlemyer, K. D. Dobson, B. E. McCandless, R. W. Birkmire, J. G. G. Chen, *Angew. Chem.* **2010**, *122*, 10055–10058; *Angew. Chem. Int. Ed.* **2010**, *49*, 9859–9862; c) Y. C. Lu, H. A. Gasteiger, Y. Shao-Horn, *J. Am. Chem. Soc.* **2011**, *133*, 19048–19051; d) I. E. L. Stephens, A. S. Bondarenko, U. Grønbjerg, J. Rossmeisl, I. Chorkendorff, *Energy Environ. Sci.* **2012**, *5*, 6744–6762.

[2] a) H. E. Hoster, M. J. Janik, M. Neurock, R. J. Behm, *Phys. Chem. Chem. Phys.* **2010**, *12*, 10388–10397; b) L. A. Kibler, A. M. El-Aziz, R. Hoyer, D. M. Kolb, *Angew. Chem.* **2005**, *117*, 2116–2120; *Angew. Chem. Int. Ed.* **2005**, *44*, 2080–2084; c) D. S. Strmcnik, D. V. Tripkovic, D. van der Vliet, K. C. Chang, V. Komanicky, H. You, G. Karapetrov, J. Greeley, V. R. Stamenkovic, N. M. Markovic, *J. Am. Chem. Soc.* **2008**, *130*, 15332–15339; d) J. L. Zhang, M. B. Vukmirovic, Y. Xu, M. Mavrikakis, R. R. Adzic, *Angew. Chem.* **2005**, *117*, 2170–2173; *Angew. Chem. Int. Ed.* **2005**, *44*, 2132–2135; e) F. J. Perez-Alonso, D. McCarthy, A. Nierhoff, P. Hernandez-Fernandez, C. Strebel, I. E. L. Stephens, J. H. Nielsen, I. Chorkendorff, *Angew. Chem.* **2012**, *124*, 4719–4721; *Angew. Chem. Int. Ed.* **2012**, *51*, 4641–4643; f) T. F. Jaramillo, K. P. Jorgensen, J. Bonde, J. H. Nielsen, S. Horch, I. Chorkendorff, *Science* **2007**, *317*, 100–102; g) P. Strasser, S. Koh, T. Anniyev, J. Greeley, K. More, C. F. Yu, Z. C. Liu, S. Kaya, D. Nordlund, H. Ogasawara, M. F. Toney, A. Nilsson, *Nat. Chem.* **2010**, *2*, 454–460.

[3] a) S. C. S. Lai, N. P. Lebedeva, T. H. M. Housmans, M. T. M. Koper, *Top. Catal.* **2007**, *46*, 320–333; b) K. J. J. Mayrhofer, M. Arenz, B. B. Blizanac, V. Stamenkovic, P. N. Ross, N. M. Markovic, *Electrochim. Acta* **2005**, *50*, 5144–5154; c) I. Kaneza-shi, S. Nohara, J. Omura, M. Watanabe, H. Uchida, *J. Electroanal. Chem.* **2011**, *662*, 123–129.

[4] J. Rossmeisl, P. Ferrin, G. A. Tritsaris, A. U. Nilekar, S. Koh, S. Brankovic, P. Strasser, M. Mavrikakis, *Energy Environ. Sci.* **2012**, DOI: 10.1039/C2EE21455E.

[5] a) J. Knudsen, A. U. Nilekar, R. T. Vang, J. Schnadt, E. L. Kunkes, J. A. Dumesic, M. Mavrikakis, F. Besenbacher, *J. Am. Chem. Soc.* **2007**, *129*, 6485–6490; b) K. J. Andersson, F. Calle-Vallejo, J. Rossmeisl, I. Chorkendorff, *J. Am. Chem. Soc.* **2009**, *131*, 2404–2407; c) I. E. L. Stephens, A. S. Bondarenko, F. J. Pérez-Alonso, F. Calle-Vallejo, L. Bech, T. P. Johansson, A. K. Jepsen, R. Frydendal, B. P. Knudsen, J. Rossmeisl, I. Chorkendorff, *J. Am. Chem. Soc.* **2011**, *133*, 5485–5491.

[6] a) A. S. Bondarenko, I. E. L. Stephens, H. A. Hansen, F. J. Pérez-Alonso, V. Tripkovic, T. P. Johansson, J. Rossmeisl, J. K. Nørskov, I. Chorkendorff, *Langmuir* **2011**, *27*, 2058–2066; b) A. Berna, V. Climent, J. M. Feliu, *Electrochem. Commun.* **2007**, *9*, 2789–2794.

[7] a) J. Greeley, M. Mavrikakis, *Catal. Today* **2006**, *111*, 52–58; b) M. P. Humbert, J. G. G. Chen, *J. Catal.* **2008**, *257*, 297–306.

[8] A. Lopez-Cudero, A. Cuesta, C. Gutierrez, *J. Electroanal. Chem.* **2005**, *579*, 1–12.

[9] D. F. van der Vliet, C. Wang, D. G. Li, A. P. Paulikas, J. Greeley, R. B. Rankin, D. Strmcnik, D. Tripkovic, N. M. Markovic, V. R. Stamenkovic, *Angew. Chem.* **2012**, *124*, 3193 – 3196; *Angew. Chem. Int. Ed.* **2012**, *51*, 3139 – 3142.

[10] a) H. Falsig, B. Hvolbaek, I. S. Kristensen, T. Jiang, T. Bligaard, C. H. Christensen, J. K. Nørskov, *Angew. Chem.* **2008**, *120*, 4913 – 4917; *Angew. Chem. Int. Ed.* **2008**, *47*, 4835 – 4839; b) P. Ferrin, A. U. Nilekar, J. Greeley, M. Mavrikakis, J. Rossmeisl, *Surf. Sci.* **2008**, *602*, 3424 – 3431.

[11] C. A. Lucas, N. M. Markovic, P. N. Ross, *Surf. Sci.* **2000**, *448*, 77 – 86.

[12] a) J. Greeley, J. K. Nørskov, *J. Phys. Chem. C* **2009**, *113*, 4932 – 4939; b) K. J. J. Mayrhofer, K. Hartl, V. Juhart, M. Arenz, *J. Am. Chem. Soc.* **2009**, *131*, 16348 – 16349; c) S. Chen, H. A. Gasteiger, K. Hayakawa, T. Tada, Y. Shao-Horn, *J. Electrochem. Soc.* **2010**, *157*, A82 – A97; d) F. J. Perez-Alonso, C. F. Elkjær, S. S. Shim, B. L. Abrams, I. E. L. Stephens, I. Chorkendorff, *J. Power Sources* **2011**, *196*, 6085 – 6091.

[13] M. Pourbaix, *Atlas of Electrochemical Equilibria in Aqueous Solutions*, 2nd ed., National Association of Corrosion Engineers, Houston, TX, **1974**.

[14] a) S. J. Yoo, S. J. Hwang, J. G. Lee, S. C. Lee, T. H. Lim, Y. E. Sung, A. Wieckowski, S. K. Kim, *Energy Environ. Sci.* **2012**, *5*, 7521 – 7525; b) S. J. Yoo, S.-K. Kim, T.-Y. Jeon, S. J. Hwang, J.-G. Lee, S.-C. Lee, K.-S. Lee, Y.-H. Cho, Y.-E. Sung, T.-H. Lim, *Chem. Commun.* **2011**, *47*, 11414 – 11416; c) X. F. Yang, J. Hu, J. Fu, R. Q. Wu, B. E. Koel, *Angew. Chem.* **2011**, *123*, 10364 – 10367; *Angew. Chem. Int. Ed.* **2011**, *50*, 10182 – 10185.

[15] a) A. A. Peterson, F. Abild-Pedersen, F. Studt, J. Rossmeisl, J. K. Nørskov, *Energy Environ. Sci.* **2010**, *3*, 1311 – 1315; b) J. K. Nørskov, J. Rossmeisl, A. Logadottir, L. Lindqvist, J. R. Kitchin, T. Bligaard, H. Jonsson, *J. Phys. Chem. B* **2004**, *108*, 17886 – 17892; c) J. K. Nørskov, T. Bligaard, A. Logadottir, J. R. Kitchin, J. G. Chen, S. Pandelov, U. Stimming, *J. Electrochem. Soc.* **2005**, *152*, J23 – J26; d) I. C. Man, H.-Y. Su, F. Calle-Vallejo, H. A. Hansen, J. I. Martínez, N. G. Inoglu, J. Kitchin, T. F. Jaramillo, J. K. Nørskov, J. Rossmeisl, *ChemCatChem* **2011**, *3*, 1159 – 1165.